Journal of chemical & engineering data

Article

pubs.acs.org/jced

Density, Viscosity, and Conductivity of Lewis Acidic 1-Butyl- and 1-Hydrogen-3-methylimidazolium Chloroaluminate Ionic Liquids

Yong Zheng,[†,‡] Kun Dong,[†,‡] Qian Wang,[†] Jianmin Zhang,[†] and Xingmei Lu*[,†]

[†]Beijing Key Laboratory of Ionic Liquids Clean Process, State Key Laboratory of Multiphase Complex Systems, Institute of Process Engineering, Chinese Academy of Sciences, Beijing 100190, P. R. China

[‡]College of Chemistry and Chemical Engineering, Graduate University of Chinese Academy of Sciences, Beijing 100049, P. R. China

ABSTRACT: To promote the development of Lewis acidic chloroaluminate ionic liquids, it is necessary to get a deeper insight into their physicochemical properties and molecular structure. In this work, the densities, viscosities, and conductivities of acidic 1-butyl- and 1-hydrogen-3-methylimidazolium chloroaluminate with different mole fractions of $AlCl_3$ were measured in the temperature range from (293.15 to 343.15) K. Meanwhile, excess molar volume and viscosity deviation values for the binary mixtures of 1-butyl-3-methylimidazolium chloroaluminate ionic liquids were also obtained. All of the experimental data were well-fitted by the empirical equations. Based on the results of density functional theory calculations, the differences in these properties are attributed to the molecular structure, cation−anion interaction, and hydrogen bonds of ionic liquids. It is expected that the present study may be deemed useful for the application of Lewis acidic chloroaluminate ionic liquids in electrochemistry and catalysis.

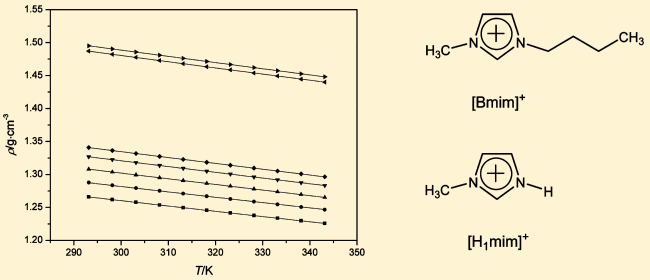

1. INTRODUCTION

Labeled as room-temperature molten salts, ionic liquids (ILs) are usually composed of organic cations and organic/inorganic anions.[1,2] Owing to the unique structure, ILs exhibit numerous excellent properties, such as a wide liquid range, negligible vapor pressure, and high electrical conductivity.[3−5] This makes ILs attractive as the potential novel materials in catalysis, electrochemistry, synthesis, and separation processes.[6−9]

In early 1950s, Hurley and Wier[10] first found that the ILs based on chloroaluminate anions could be formed by the combination of *N*-ethylpyridinium chloride with $AlCl_3$. Since then, extensive research on the chloroaluminate ILs has been reported in the literature.[11−15] It is demonstrated that the acidity of these ILs is adjustable by varying the molar ratio of organic chloride salt ([R]Cl) to $AlCl_3$. When the apparent mole fraction, x, of $AlCl_3$ is higher than 0.5, the ILs are acidic due to an excess of Lewis acidic $AlCl_3$. The most widely studied apparent mole fraction range of $AlCl_3$ is 0.50 to 0.66, and the main species of Lewis acidic anions are confirmed as $[Al_2Cl_7]^-$ (see eqs 1 and 2) in these ILs.[16,17] The relatively high conductivity, wide electrochemical window, and tunable acidity render these ILs as potential electrolytes and catalysts. Although Lewis acidic chloroaluminate ILs have been widely applied in the low-temperature metal electrodeposition and organic synthesis over the past decades,[18−21] the investigation on their physicochemical and structural properties is still limited. From the perspective of fundamental research and industrial application, it is necessary to make further exploration of the relationship between these properties.

$$Cl^- + AlCl_3 \rightarrow [AlCl_4]^- \quad (1)$$

$$[AlCl_4]^- + AlCl_3 \rightarrow [Al_2Cl_7]^- \quad (2)$$

In our previous work, two typical series of Lewis acidic imidazolium chloroaluminate ILs: 1-butyl-3-methylimidazolium chloroaluminate ([Bmim]Cl/$AlCl_3$) and 1-hydrogen-3-methylimidazolium chloroaluminate ([H_1mim]Cl/$AlCl_3$) were used as novel electrolytes (see Figure 1). It shows that these ILs have a bright prospect in the low-temperature electrodeposition of aluminum.[16,22,23] Nevertheless, a literature survey reveals that only the physicochemical properties of [Bmim]Cl/$AlCl_3$ (x = 0.66) have been studied.[24,25] No literature reported a systematic study on the structural, thermodynamic, and electrochemical features of above Lewis acidic ILs. Therefore, in this paper, the densities, viscosities, and electrical conductivities of acidic [Bmim]Cl/$AlCl_3$ and [H_1mim]Cl/$AlCl_3$ have been measured at different conditions. The excess molar volume and viscosity deviation for the binary mixtures of [Bmim]-[$AlCl_4$] and [Bmim][Al_2Cl_7] were also obtained. Based on molecular simulation, the experimental results were discussed from the ionic structure, cation−anion interaction, and hydrogen

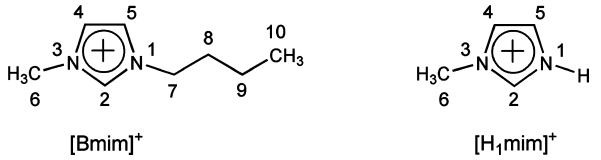

Figure 1. Structure of imidazolium cations studied in this work.

Received: June 8, 2012
Accepted: November 13, 2012
Published: November 27, 2012

bonds of ILs. The present study can be useful in simultaneous understanding of physicochemical properties and correlation with the molecular structure of Lewis acidic chloroaluminate ILs.

2. EXPERIMENTAL SECTION

2.1. Chemicals. All of the chemicals used in this work were purchased commercially with analytic grade from Alfa Aesar and Sinopharm Chemical Reagent Co., Ltd. *N*-Methylimidazolium (mass fraction ≥ 99 %), 1-chlorobutane (mass fraction > 99.5 %), ethyl acetate (mass fraction > 99.5 %), and acetone (mass fraction > 99.5 %) were purified by distillation. Anhydrous aluminum chloride (mass fraction ≥ 99 %) and hydrochloric acid (HCl mass fraction 36 to 38 %) were used without further purification.

Table 1. Comparison of the Density, Viscosity, and Electrical Conductivity of [Bmim]Cl/$AlCl_3$ (x = 0.6667) Measured in This Work with Literature Values[a]

	ρ (g·cm^{-3})		η (mPa·s)		κ (mS·cm^{-1})	
T/K	this work	lit.[24]	this work	lit.[24]	this work	lit.[24]
298.15	1.336321	1.334	19.42	19.3	9.12	9.2
318.15	1.318436	1.316	11.35	11.3	14.99	15.1
338.15	1.300828	1.299	7.433	7.4	21.96	22.0

[a]The composition x is the apparent mole fraction of $AlCl_3$ in [Bmim]Cl/$AlCl_3$. Standard uncertainties u are $u(x)$ = 0.0001, $u(T)$ = (0.01, 0.01, and 0.05) K for ρ, η, and κ, respectively, the expanded uncertainties for the densities $U(\rho) = 3\cdot10^{-5}$ g·cm^{-3}, and the relative expanded uncertainties for the viscosities $U_r(\eta)$ and electrical conductivities $U_r(\kappa)$ are 0.005 (level of confidence = 0.95).

2.2. Synthesis of ILs. *[Bmim]Cl (1-Butyl-3-methylimidazolium Chloride).* According to the literature,[26] equimolar amounts of 1-chlorobutane and *N*-methylimidazolium were stirred in a flask for 48 h at 343 K. The mixture was then washed by ethyl acetate, recrystallized from acetone, and dried under vacuum. The final product was obtained as a white wax-like solid at room temperature. ^{1}H NMR: δ = 9.446 (s, 1H), 7.840 (d, 1H), 7.765 (d, 1H), 4.177 (t, 2H), 3.856 (s, 3H), 1.747 (m, 2H), 1.233 (m, 2H), and 0.873 (m, 3H) ppm. Elemental analysis: C (54.89 wt %), N (16.01 wt %), H (8.56 wt %), and Cl (20.28 wt %).

[H_1mim]Cl (1-Hydrogen-3-methylimidazolium Chloride). As Ohno et al.[27] described, 1.1 mol of hydrochloric acid was added dropwise into 1 mol of *N*-methylimidazolium under stirring at 273 K. Then, the mixture was heated up to 333 K and stirred for 6 h. After the resulting solution was concentrated by rotary evaporation, the residual liquid was washed by acetone and dried under vacuum at 343 K for 48 h. The final product was obtained as a colorless solid at room temperature. ^{1}H NMR: δ = 12.402 (s, 1H), 9.286 (s, 1H), 7.793 (d, 1H), 7.691 (d, 1H), and 3.927 (s, 3H) ppm. Elemental analysis: C (40.41 wt %), N (23.58 wt %), H (5.90 wt %), and Cl (29.85 wt %).

Lewis [Bmim]Cl/$AlCl_3$. The preparation and subsequent purification processes were all conducted in an argon-filled glovebox (Universal, MIKROUNA Co., China) where water and oxygen content was both kept below 1 ppm. Lewis [Bmim]Cl/$AlCl_3$ with different apparent mole fractions, x, of $AlCl_3$ (x = 0.5000, 0.5455, 0.5833, 0.6154, 0.6429 and 0.6667) were synthesized by mixing precise molar quantities of [Bmim]Cl with anhydrous $AlCl_3$ at the molar ratios of 1:1.0, 1:1.2, 1:1.4, 1:1.6, 1:1.8, and 1:2.0, respectively.[22] The resulting liquids were filtered through glass frit and purified by electrolysis before use. The final products were obtained as colorless liquids at room temperature. The standard uncertainty $u(x)$ is 0.0001. ^{1}H NMR of

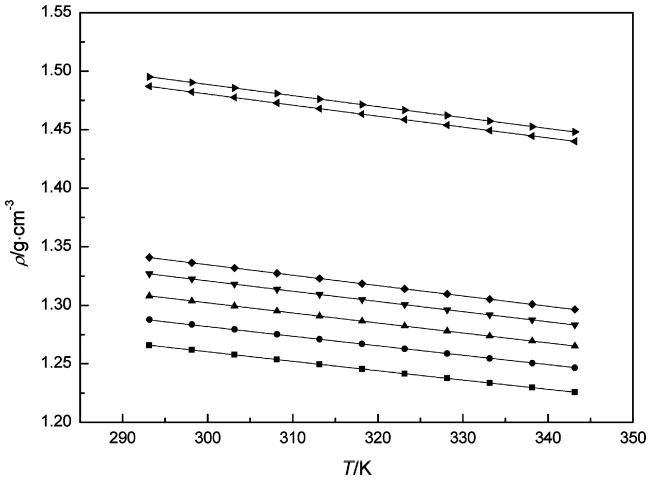

Figure 2. Temperature dependence on the density of Lewis acidic [Bmim]Cl/$AlCl_3$ and [H_1mim]Cl/$AlCl_3$. [Bmim]Cl/$AlCl_3$: ■, x = 0.5455; ●, x = 0.5833; ▲, x = 0.6154; ▼, x = 0.6429; ◆, x = 0.6667. [H_1mim]Cl/$AlCl_3$: ◀, x = 0.6429; ▶, x = 0.6667. The composition x is the apparent mole fraction of $AlCl_3$ in [Bmim]Cl/$AlCl_3$ and [H_1mim]Cl/$AlCl_3$.

Table 2. Experimental Density, ρ (g·cm^{-3}), of Lewis Acidic [Bmim]Cl/$AlCl_3$ and [H_1mim]Cl/$AlCl_3$ ILs[a]

	[Bmim]Cl/$AlCl_3$					[H_1mim]Cl/$AlCl_3$	
T/K	x = 0.5455	x = 0.5833	x = 0.6154	x = 0.6429	x = 0.6667	x = 0.6429	x = 0.6667
293.15	1.265918	1.287782	1.307946	1.326919	1.340883	1.487071	1.495185
298.15	1.261813	1.283583	1.303622	1.322476	1.336321	1.482258	1.490335
303.15	1.257730	1.279396	1.299320	1.318051	1.331806	1.477510	1.485655
308.15	1.253668	1.275230	1.295035	1.313645	1.327321	1.472778	1.480895
313.15	1.249623	1.271085	1.290767	1.309259	1.322868	1.468037	1.476200
318.15	1.245597	1.266955	1.286508	1.304890	1.318436	1.463342	1.471480
323.15	1.241593	1.262847	1.282267	1.300535	1.314007	1.458636	1.466775
328.15	1.237615	1.258749	1.278025	1.296192	1.309593	1.453944	1.462076
333.15	1.233646	1.254665	1.273776	1.291873	1.305206	1.449284	1.457383
338.15	1.229698	1.250587	1.269506	1.287556	1.300828	1.444646	1.452697
343.15	1.225755	1.246505	1.265203	1.283228	1.296477	1.440044	1.448145

[a]The composition x is the apparent mole fraction of $AlCl_3$ in [Bmim]Cl/$AlCl_3$ and [H_1mim]Cl/$AlCl_3$. Standard uncertainties u are $u(T)$ = 0.01 K, $u(x)$ = 0.0001, and the expanded uncertainties for the densities $U(\rho) = 3\cdot10^{-5}$ g·cm^{-3} (level of confidence = 0.95).

dx.doi.org/10.1021/je3004904 | J. Chem. Eng. Data 2013, 58, 32−42

[Bmim]Cl/$AlCl_3$ (x = 0.5000): δ = 8.330 (s, 1H), 7.304 (d, 1H), 7.266 (d, 1H), 4.087 (t, 2H), 3.829 (s, 3H), 1.771 (m, 2H), 1.252 (m, 2H), and 0.791 (m, 3H) ppm. Elemental analysis of [Bmim]Cl/$AlCl_3$ (x = 0.5000): C (31.05 wt %), N (9.07 wt %), H (4.85 wt %), and Cl (45.98 wt %). ^{1}H NMR of [Bmim]Cl/$AlCl_3$ (x = 0.5455): δ = 8.307 (s, 1H), 7.292 (d, 1H), 7.255 (d, 1H), 4.080 (t, 2H), 3.824 (s, 3H), 1.768 (m, 2H), 1.249 (m, 2H), and 0.790 (m, 3H) ppm. Elemental analysis of [Bmim]Cl/$AlCl_3$ (x = 0.5455): C (28.64 wt %), N (8.35 wt %), H (4.47 wt %), and Cl (48.62 wt %).

Table 3. Fitted Values of the Empirical Parameters, *A*, *B*, and *C* for the Density of Lewis Acidic [Bmim]Cl/$AlCl_3$ and [H_1mim]Cl/$AlCl_3$ ILs Based on eq 3[a]

x	A / g·cm^{-3}	10^3B / g·cm^{-3}·K^{-1}	10^7C / g·cm^{-3}·K^{-2}	R^2
		[Bmim]Cl/$AlCl_3$		
0.5455	1.53965	−1.05138	3.81027	0.9999
0.5833	1.56163	−1.04578	3.57325	0.9998
0.6154	1.58823	−1.03984	2.88359	0.9999
0.6429	1.60766	−1.03146	2.46382	0.9999
0.6667	1.62031	−1.01435	1.92609	0.9999
		[H_1mim]Cl/$AlCl_3$		
0.6429	1.80183	−1.19247	3.95962	0.9999
0.6667	1.80739	−1.17152	3.63237	0.9999

[a]The composition x is the apparent mole fraction of $AlCl_3$ in [Bmim]Cl/$AlCl_3$ and [H_1mim]Cl/$AlCl_3$.

^{1}H NMR of [Bmim]Cl/$AlCl_3$ (x = 0.5833): δ = 8.274 (s, 1H), 7.271 (d, 1H), 7.237 (d, 1H), 4.071 (t, 2H), 3.817 (s, 3H), 1.763 (m, 2H), 1.245 (m, 2H), and 0.787 (m, 3H) ppm. Elemental analysis of [Bmim]Cl/$AlCl_3$ (x = 0.5833): C (26.55 wt %), N (7.73 wt %), H (4.14 wt %), and Cl (50.95 wt %). ^{1}H NMR of [Bmim]Cl/$AlCl_3$ (x = 0.6154): δ = 8.208 (s, 1H), 7.223 (d, 1H), 7.191 (d, 1H), 4.036 (t, 2H), 3.784 (s, 3H), 1.734 (m, 2H), 1.224 (m, 2H), and 0.772 (m, 3H) ppm. Elemental analysis of [Bmim]Cl/$AlCl_3$ (x = 0.6154): C (24.72 wt %), N (7.19 wt %), H (3.86 wt %), and Cl (52.87 wt %). ^{1}H NMR of [Bmim]Cl/$AlCl_3$ (x = 0.6429): δ = 8.096 (s, 1H), 7.138 (d, 1H), 7.108 (d, 1H), 3.972 (t, 2H), 3.722 (s, 3H), 1.683 (m, 2H), 1.184 (m, 2H), and 0.746 (m, 3H) ppm. Elemental analysis of [Bmim]Cl/$AlCl_3$ (x = 0.6429): C (23.13 wt %), N (6.74 wt %), H (3.61 wt %), and Cl (54.58 wt %). ^{1}H NMR of [Bmim]Cl/$AlCl_3$ (x = 0.6667): δ = 7.931 (s, 1H), 6.997 (d, 1H), 6.969 (d, 1H), 3.858 (t, 2H), 3.610 (s, 3H), 1.599 (m, 2H), 1.118 (m, 2H), and 0.697 (m, 3H) ppm. ^{27}Al NMR of [Bmim]Cl/$AlCl_3$ (x = 0.6667): δ = 106.626 ppm. Elemental analysis of [Bmim]Cl/$AlCl_3$ (x = 0.6667): C (21.72 wt %), N (6.33 wt %), H (3.39 wt %), and Cl (56.13 wt %). In the determination of excess volumes and viscosity deviation, the systems used were prepared by mixing precise molar quantities of [Bmim]Cl/$AlCl_3$ (x = 0.5000) and [Bmim]Cl/$AlCl_3$ (x = 0.6667) at room temperature.

Lewis Acidic [H_1mim]Cl/$AlCl_3$. These ILs were synthesized and purified in the same way as described above for [Bmim]Cl/$AlCl_3$. However, it was found that [H_1mim]Cl/$AlCl_3$ remained

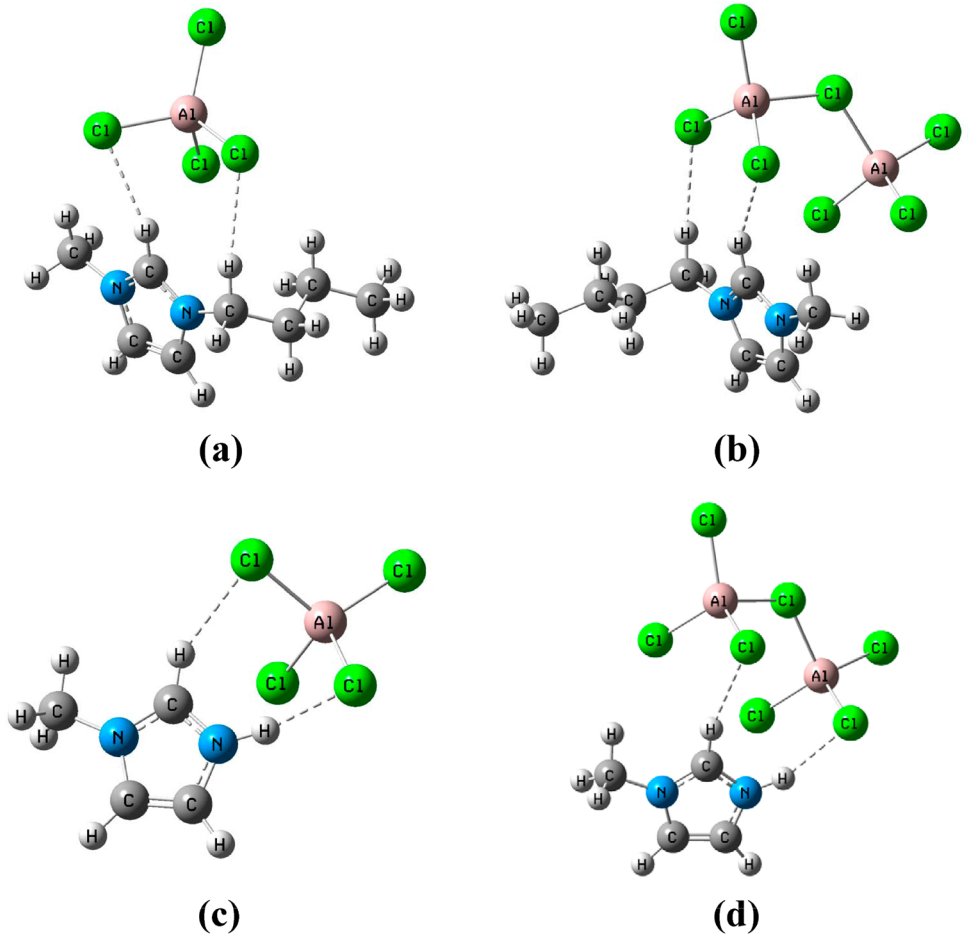

Figure 3. Optimized geometries of (a) [Bmim][$AlCl_4$], (b) [Bmim][Al_2Cl_7], (c) [H_1mim][$AlCl_4$], and (d) [H_1mim][Al_2Cl_7] at B3LYP/6-31+G(d,p) level. Hydrogen bonds are indicated by dashed lines.

dx.doi.org/10.1021/je3004904 | J. Chem. Eng. Data 2013, 58, 32−42

solid below 303 K when the apparent mole fraction of $AlCl_3$ was lower than 0.64. To facilitate the following measurement of physicochemical properties, only the $[H_1mim]Cl/AlCl_3$ ILs with 0.6429 and 0.6667 apparent mole fraction, x, of $AlCl_3$ were used. The standard uncertainty $u(x)$ is 0.0001. ^1H NMR of $[H_1mim]Cl/AlCl_3$ (x = 0.6429): δ = 10.355 (s, 1H), 8.297 (s, 1H), 7.328 (d, 1H), 7.247 (d, 1H), and 3.845 (s, 3H) ppm. Elemental analysis of $[H_1mim]Cl/AlCl_3$ (x = 0.6429): C (13.36 wt %), N (7.79 wt %), H (1.94 wt %), and Cl (63.16 wt %). ^1H NMR of $[H_1mim]Cl/AlCl_3$ (x = 0.6667): δ = 10.102 (s, 1H), 8.099 (s, 1H), 7.108 (d, 1H), 7.025 (d, 1H), and 3.618 (s, 3H) ppm. ^{27}Al NMR of $[H_1mim]Cl/AlCl_3$ (x = 0.6667): δ = 99.531 ppm. Elemental analysis of $[H_1mim]Cl/AlCl_3$ (x = 0.6667): C (12.43 wt %), N (7.25 wt %), H (1.81 wt %), and Cl (64.42 wt %).

2.3. Characterization of ILs. ^1H NMR, ^{27}Al NMR, elemental analysis, and water content analysis were performed to identify the structure and purity of ILs. The NMR spectra of [Bmim]Cl and $[H_1mim]Cl$ were recorded on a NMR spectrometer (av-400 MHz, Bruker, Switzerland) in DMSO-d_6 at 298 K. In the NMR measurements of $[Bmim]Cl/AlCl_3$ and $[H_1mim]Cl/AlCl_3$, acetone-d_6 was used as an external standard to suppress the interference from other solvents. The elemental analysis of ILs was conducted with an elemental analyzer (Vario El cube, Elementar, Germany).

All of the peaks and corresponding chemical shifts obtained confirmed the structure of these ILs, and no impurity peaks were found in the NMR spectra. The results of elemental analysis fitted well with the composition of ILs. Analyzed by Karl Fisher titration (751 GPD Titrino, Metrohm, Switzerland), the water content of [Bmim]Cl and $[H_1mim]Cl$ was less than 150 ppm in mass. For $[Bmim]Cl/AlCl_3$ and $[H_1mim]Cl/AlCl_3$,

Table 4. Calculated Parameters of $[Bmim][AlCl_4]$, $[Bmim][Al_2Cl_7]$, $[H_1mim][AlCl_4]$, and $[H_1mim][Al_2Cl_7]$ Ion Pairs at B3LYP/6-31+G(d,p) Level

IL	ΔE^a / KJ·mol^{-1}	μ^b / D	C2−H···Cl^c / Å	C7−H···Cl^c / Å	N1−H···Cl^c / Å
[Bmim][$AlCl_4$]	290.98	15.32	2.588	2.697	
[Bmim][Al_2Cl_7]	270.61	15.56	2.616	2.725	
[H_1mim][$AlCl_4$]	318.36	13.87	2.486		2.115
[H_1mim][Al_2Cl_7]	295.90	14.25	2.510		2.236

[a]The interaction energy of ion pairs. [b]The dipole moment of ion pairs. [c]The distance of hydrogen bond between H and Cl atoms.

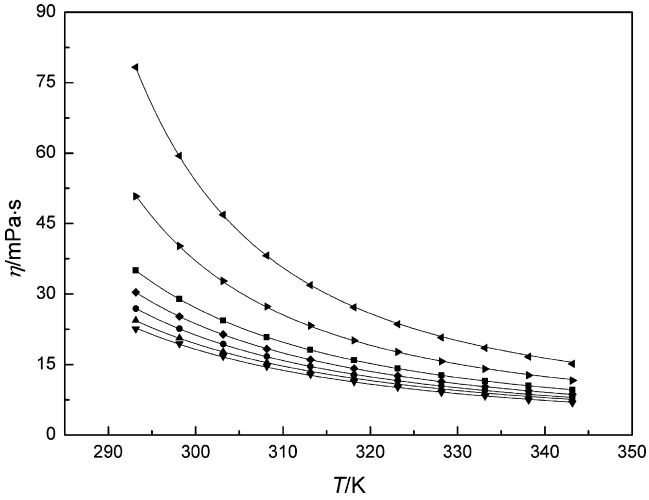

Figure 4. Temperature dependence on the viscosity of Lewis acidic $[Bmim]Cl/AlCl_3$ and $[H_1mim]Cl/AlCl_3$. $[Bmim]Cl/AlCl_3$: ■, x = 0.5455; ◆, x = 0.5833; ●, x = 0.6154; ▲, x = 0.6429; ▼, x = 0.6667. $[H_1mim]Cl/AlCl_3$: ◀, x = 0.6429; ▶, x = 0.6667. The composition x is the apparent mole fraction of $AlCl_3$ in $[Bmim]Cl/AlCl_3$ and $[H_1mim]Cl/AlCl_3$.

Table 6. Fitted Values of the Empirical Parameters, η_0, B, and T_0 for the Viscosity of Lewis Acidic $[Bmim]Cl/AlCl_3$ and $[H_1mim]Cl/AlCl_3$ ILs Based on VFT Equation[a]

x	η_0 / mPa·s	B / K	T_0 / K	R^2
		$[Bmim]Cl/AlCl_3$		
0.5455	0.990	314.0	205.1	0.9999
0.5833	0.865	325.7	201.6	0.9999
0.6154	0.776	338.6	197.8	0.9998
0.6429	0.730	351.1	193.0	0.9999
0.6667	0.547	403.2	185.7	0.9995
		$[H_1mim]Cl/AlCl_3$		
0.6429	2.298	206.0	234.6	0.9999
0.6667	1.670	227.1	227.6	0.9999

[a]The composition x is the apparent mole fraction of $AlCl_3$ in $[Bmim]Cl/AlCl_3$ and $[H_1mim]Cl/AlCl_3$.

Table 5. Experimental Viscosity, η (mPa·s), of Lewis Acidic $[Bmim]Cl/AlCl_3$ and $[H_1mim]Cl/AlCl_3$ ILs[a]

	$[Bmim]Cl/AlCl_3$					$[H_1mim]Cl/AlCl_3$	
T/K	x = 0.5455	x = 0.5833	x = 0.6154	x = 0.6429	x = 0.6667	x = 0.6429	x = 0.6667
293.15	35.03	30.36	26.91	24.38	22.54	78.29	50.80
298.15	28.92	25.24	22.59	20.62	19.42	59.41	40.23
303.15	24.35	21.38	19.34	17.70	16.73	46.88	32.79
308.15	20.84	18.38	16.72	15.39	14.59	38.17	27.36
313.15	18.10	16.03	14.61	13.54	12.87	31.87	23.28
318.15	15.92	14.15	12.88	12.04	11.35	27.17	20.13
323.15	14.15	12.61	11.56	10.80	10.17	23.58	17.66
328.15	12.70	11.34	10.45	9.758	9.046	20.75	15.67
333.15	11.49	10.29	9.497	8.884	8.231	18.50	14.06
338.15	10.48	9.395	8.691	8.140	7.433	16.67	12.72
343.15	9.627	8.636	8.013	7.501	6.824	15.15	11.61

[a]The composition x is the apparent mole fraction of $AlCl_3$ in $[Bmim]Cl/AlCl_3$ and $[H_1mim]Cl/AlCl_3$. Standard uncertainties u are $u(T)$ = 0.01 K, $u(x)$ = 0.0001, and the relative expanded uncertainties for the viscosities $U_r(\eta)$ = 0.005 (level of confidence = 0.95).

dx.doi.org/10.1021/je3004904 | J. Chem. Eng. Data 2013, 58, 32−42

Table 7. Electrical Conductivity, κ (mS·cm^{-1}), of Lewis Acidic [Bmim]Cl/$AlCl_3$ and [H_1mim]Cl/$AlCl_3$ ILs[a]

	[Bmim]Cl/$AlCl_3$					[H_1mim]Cl/$AlCl_3$	
T/K	x = 0.5455	x = 0.5833	x = 0.6154	x = 0.6429	x = 0.6667	x = 0.6429	x = 0.6667
298.15	9.80	9.47	9.31	9.19	9.12	4.54	6.01
303.15	11.44	10.96	10.73	10.60	10.51	5.53	7.09
308.15	13.21	12.64	12.28	12.07	11.95	6.61	8.27
313.15	15.11	14.39	13.87	13.61	13.44	7.82	9.61
318.15	17.13	16.27	15.75	15.22	14.99	9.09	10.98
323.15	19.26	18.31	17.56	16.93	16.61	10.49	12.45
328.15	21.51	20.38	19.48	18.76	18.30	11.98	14.02
333.15	23.86	22.62	21.62	20.72	20.08	13.58	15.65
338.15	26.31	24.93	23.79	22.81	21.96	15.26	17.38
343.15	28.84	27.29	26.05	24.97	23.95	17.03	19.23

[a]The composition x is the apparent mole fraction of $AlCl_3$ in [Bmim]Cl/$AlCl_3$ and [H_1mim]Cl/$AlCl_3$. Standard uncertainties u are $u(T)$ = 0.05 K, $u(x)$ = 0.0001, and the relative expanded uncertainties for the electrical conductivities $U_r(\kappa)$ = 0.005 (level of confidence = 0.95).

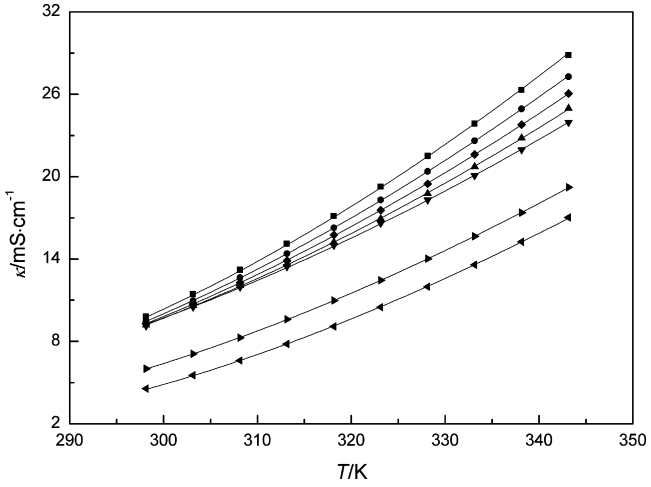

Figure 5. Temperature dependence on the electrical conductivity of Lewis acidic [Bmim]Cl/$AlCl_3$ and [H_1mim]Cl/$AlCl_3$. [Bmim]Cl/$AlCl_3$: ■, x = 0.5455; ●, x = 0.5833; ◆, x = 0.6154; ▲, x = 0.6429; ▼, x = 0.6667. [H_1mim]Cl/$AlCl_3$: ◀, x = 0.6429; ▶, x = 0.6667. The composition x is the apparent mole fraction of $AlCl_3$ in [Bmim]Cl/$AlCl_3$ and [H_1mim]Cl/$AlCl_3$.

Table 8. Fitted Values of the Empirical Parameters, κ_0, B, and T_0 for the Electrical Conductivity of Lewis Acidic [Bmim]Cl/$AlCl_3$ and [H_1mim]Cl/$AlCl_3$ ILs Based on VFT Equation[a]

	κ_0	B	T_0	
x	S·cm^{-1}	K	K	R^2
		[Bmim]Cl/$AlCl_3$		
0.5455	0.94	656.9	154.3	0.9998
0.5833	0.91	678.8	149.5	0.9999
0.6154	0.89	703.9	143.8	0.9999
0.6429	0.88	735.4	136.9	0.9999
0.6667	0.87	771.3	128.4	0.9998
		[H_1mim]Cl/$AlCl_3$		
0.6429	0.39	474.3	191.8	0.9999
0.6667	0.52	569.2	170.6	0.9999

[a]The composition x is the apparent mole fraction of $AlCl_3$ in [Bmim]Cl/$AlCl_3$ and [H_1mim]Cl/$AlCl_3$.

the results of measurement showed that the water content was below 50 ppm. According to these measurements, the mass fraction purity of all of the ILs was determined to be > 99 %.

2.4. Density Measurements. The densities of ILs were measured by a high-precision vibrating tube densimeter (Anton Paar DMA 5000, Anton Paar Co., Austria) with expanded uncertainty $U(\rho) = 3\cdot10^{-5}$ g·cm^{-3} (0.95 level of confidence) in the argon-filled glovebox. Prior to measurement, the densimeter was calibrated with ultrapure water and dry air. The measuring temperature range was from (293.15 to 343.15) K. Controlled by two integrated Pt 100 platinum thermometers, the precision of temperature was as high as ± 0.001 K.

2.5. Viscosity Measurements. For the viscosity measurements of ILs, an automated microviscometer (Anton Paar AMVn, Anton Paar Co., Austria) with relative expanded uncertainty $U_r(\eta)$ = 0.005 (0.95 level of confidence) was used. Calibration was performed using ultrapure water or viscosity standard oils (No. H117, Anton Paar Co.). The measurements were conducted in the argon-filled glovebox. The temperature of this study ranged from (293.15 to 343.15) K, which was controlled by a built-in precise Peltier thermostat with an accuracy of ± 0.01 K.

2.6. Electrical Conductivity Measurements. The electrical conductivities of ILs were obtained through a conductivity meter (FE30, Mettler Toledo Int. Inc., Switzerland) equipped with a conductivity probe (InLab 710, Mettler Toledo Int. Inc., Switzerland) in the argon-filled glovebox. The relative expanded uncertainty $U_r(\kappa)$ for these measurements is 0.005 (0.95 level of confidence). The values were recorded in the temperature range from (298.15 to 343.15) K. The experimental temperature was controlled by a thermostat with an accuracy of ± 0.05 K. At each given temperature, the time for attaining thermal equilibrium was more than 0.5 h.

2.7. Computational Methods. Based on density functional theory (DFT), all of the calculations for ILs were performed with the Guassian09 program. The geometries of all of the studied ion pairs were optimized using Becke−three-parameter−Lee−Yang−Parr (B3LYP) with 6-31+G(d,p) basis set. Each optimized structure was checked to be a true minimum by frequency calculation at the corresponding level. Basis set superposition errors (BSSE) were considered for interaction energy through the counterpoise method.

The experimental and literature data of [Bmim]Cl/$AlCl_3$ (x = 0.6667) at some typical temperatures have been listed in Table 1. The overall average relative error of density, viscosity, and electrical conductivity of [Bmim]Cl/$AlCl_3$ (x = 0.6667) between this work and literature is less than 0.22 %, 0.79 %, and 0.88 %, respectively. It shows that our experimental data are in good agreement with literature values.

dx.doi.org/10.1021/je3004904 | J. Chem. Eng. Data 2013, 58, 32−42

Table 9. Molar Conductivity, Λ (S·cm²·mol⁻¹), of Lewis Acidic [Bmim]Cl/$AlCl_3$ and [H_1mim]Cl/$AlCl_3$ ILs[a]

	[Bmim]Cl/$AlCl_3$					[H_1mim]Cl/$AlCl_3$	
T/K	x = 0.5455	x = 0.5833	x = 0.6154	x = 0.6429	x = 0.6667	x = 0.6429	x = 0.6667
298.15	2.60	2.67	2.77	2.88	3.01	1.10	1.55
303.15	3.04	3.09	3.20	3.33	3.48	1.34	1.84
308.15	3.53	3.58	3.68	3.81	3.97	1.61	2.15
313.15	4.05	4.09	4.17	4.31	4.48	1.91	2.51
318.15	4.60	4.64	4.75	4.84	5.02	2.23	2.87
323.15	5.19	5.24	5.31	5.40	5.58	2.58	3.27
328.15	5.82	5.85	5.91	6.00	6.17	2.95	3.69
333.15	6.47	6.51	6.58	6.65	6.79	3.36	4.14
338.15	7.16	7.20	7.27	7.34	7.45	3.79	4.61
343.15	7.87	7.91	7.99	8.07	8.15	4.24	5.11

[a]The composition x is the apparent mole fraction of $AlCl_3$ in [Bmim]Cl/$AlCl_3$ and [H_1mim]Cl/$AlCl_3$. Standard uncertainties u are u(T) = 0.05 K, u(x) = 0.0001, and the relative expanded uncertainties for the molar conductivities $U_r(\Lambda)$ = 0.006 (level of confidence = 0.95).

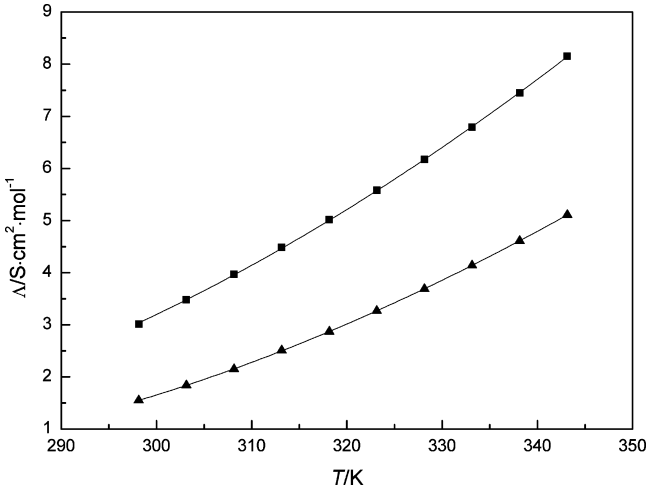

Figure 6. Temperature dependence on the molar conductivity of Lewis acidic ILs: ■, [Bmim]Cl/$AlCl_3$ (x = 0.6667); ▲, [H_1mim]Cl/$AlCl_3$ (x = 0.6667). The composition x is the apparent mole fraction of $AlCl_3$ in [Bmim]Cl/$AlCl_3$ and [H_1mim]Cl/$AlCl_3$.

Table 10. Fitted Values of the Empirical Parameters, Λ_0, B, and T_0 for the Molar Conductivity of Lewis Acidic [Bmim]Cl/$AlCl_3$ and [H_1mim]Cl/$AlCl_3$ ILs Based on VFT Equation[a]

	Λ_0	B	T_0	
x	S·cm²·mol⁻¹	K	K	R^2
		[Bmim]Cl/$AlCl_3$		
0.5455	222.30	603.53	162.49	0.9999
0.5833	231.49	619.33	159.63	0.9999
0.6154	241.13	644.67	154.08	0.9999
0.6429	253.04	675.68	147.31	0.9998
0.6667	268.47	715.22	138.55	0.9999
		[H_1mim]Cl/$AlCl_3$		
0.6429	162.59	608.13	176.39	0.9999
0.6667	175.35	631.27	164.63	0.9999

[a]The composition x is the apparent mole fraction of $AlCl_3$ in [Bmim]Cl/$AlCl_3$ and [H_1mim]Cl/$AlCl_3$.

3. RESULTS AND DISCUSSION

3.1. Density. The densities, ρ, of Lewis acidic chloroaluminate ILs measured from (293.15 to 343.15) K have been presented in Table 2. As Figure 2 illustrates, the density values fit well with experimental temperature T according to the following equation:[28,29]

$$\rho = A + BT + CT^2 \quad (3)$$

where A (g·cm⁻³), B (g·cm⁻³·K⁻¹), and C (g·cm⁻³·K⁻²) are adjustable parameters. The best fitted parameters are listed in Table 3.

As expected, the densities of these ILs slightly decrease with increasing temperature. This phenomenon reflects that the increase in temperature results in a reduction of ILs volume and number of ions per unit volume. Meanwhile, the densities of ILs follow the order: [Bmim]Cl/$AlCl_3$ (x = 0.5455) < [Bmim]Cl/$AlCl_3$ (x = 0.5833) < [Bmim]Cl/$AlCl_3$ (x = 0.6154) < [Bmim]Cl/$AlCl_3$ (x = 0.6429) < [Bmim]Cl/$AlCl_3$ (x = 0.6667), and [H_1mim]Cl/$AlCl_3$ (x = 0.6429) < [H_1mim]Cl/$AlCl_3$ (x = 0.6667) at the same temperature. For [R]Cl/$AlCl_3$ ILs (x = 0.50 and 0.66), it is well-known that the predominant presence of anions can be expressed as $[AlCl_4]^-$ and $[Al_2Cl_7]^-$, respectively.[16] The molar concentration of $[Al_2Cl_7]^-$ is enhanced when the apparent mole fraction of $AlCl_3$ increases from 0.50 to 0.66, indicating that above order is mainly attributed to the increasing molar concentration of heavier formula weight anion ($[Al_2Cl_7]^-$) in [Bmim]Cl/$AlCl_3$ and [H_1mim]Cl/$AlCl_3$.

In this work, the densities of [H_1mim]Cl/$AlCl_3$ are found to be much higher than those of [Bmim]Cl/$AlCl_3$ at the same conditions. It can be inferred that the species of cation have an important effect on the density of IL. To illustrate the relationship between molecular structure and properties of these ILs, the optimized geometries, structural parameters, hydrogen bonds, dipole moment, and interaction energy of four ion pairs have been calculated by DFT (see Figure 3 and Table 4). According to these results, [H_1mim][Al_2Cl_7] and [H_1mim][$AlCl_4$] have a smaller molecular size and higher structural symmetry than [Bmim]-[Al_2Cl_7] and [Bmim][$AlCl_4$] when these ion pairs contain the same anions. Therefore, it is easy to understand that the structural features of [H_1mim]⁺-based ion pairs promote the close packing of ions in Lewis acidic [H_1mim]Cl/$AlCl_3$. As a result, [H_1mim]Cl/$AlCl_3$ are much denser than [Bmim]Cl/$AlCl_3$.

3.2. Viscosity. The viscosities, η, determined for Lewis acidic [Bmim]Cl/$AlCl_3$ and [H_1mim]Cl/$AlCl_3$ are given in Table 5. Figure 4 shows the temperature dependency of the viscosity for these ILs. The values of viscosity were fitted by the Vogel–Fulcher–Tamman (VFT) equation, which is often used for ILs:

$$\eta = \eta_0 \exp(B/(T - T_0)) \quad (4)$$

dx.doi.org/10.1021/je3004904 | J. Chem. Eng. Data 2013, 58, 32–42

Table 11. Experimental Density, ρ (g·cm^{-3}), and Excess Molar Volume, V^E (cm^3·mol^{-1}), for the Binary Mixture of [Bmim][Al_2Cl_7] (1) + [Bmim][$AlCl_4$] (2)[a]

	T/K					
x_1	293.15	303.15	313.15	323.15	333.15	343.15
			ρ/g·cm^{-3}			
0.0000	1.242174	1.234347	1.226587	1.218892	1.211253	1.203681
0.1001	1.254063	1.246052	1.238113	1.230234	1.222402	1.214624
0.1998	1.265526	1.257369	1.249291	1.241268	1.233283	1.225342
0.3003	1.276820	1.268519	1.260309	1.252167	1.244075	1.236018
0.4002	1.287554	1.279124	1.270789	1.262516	1.254294	1.246129
0.5009	1.297823	1.289264	1.280803	1.272410	1.264065	1.255781
0.6001	1.307375	1.298721	1.290169	1.281687	1.273259	1.264889
0.7000	1.316517	1.307735	1.299072	1.290474	1.281928	1.273437
0.8005	1.325120	1.316240	1.307485	1.298805	1.290182	1.281623
0.8996	1.333153	1.324173	1.315324	1.306549	1.297834	1.289190
1.0000	1.340883	1.331806	1.322868	1.314007	1.305206	1.296477
			V^E/cm^3·mol^{-1}			
0.1001	0.1654	0.1734	0.1823	0.1928	0.2056	0.2216
0.1998	0.2545	0.2636	0.2739	0.2872	0.3050	0.3286
0.3003	0.2513	0.2613	0.2717	0.2825	0.2953	0.3159
0.4002	0.2138	0.2226	0.2326	0.2448	0.2588	0.2759
0.5009	0.1634	0.1721	0.1831	0.1952	0.2099	0.2270
0.6001	0.1170	0.1197	0.1252	0.1315	0.1390	0.1496
0.7000	0.0635	0.0687	0.0743	0.0823	0.0921	0.1061
0.8005	0.0377	0.0398	0.0424	0.0451	0.0484	0.0536
0.8996	0.0178	0.0189	0.0204	0.0225	0.0246	0.0268

[a]The composition x_1 is the mole fraction of [Bmim][Al_2Cl_7] in the binary mixture. Standard uncertainties u are $u(T)$ = 0.01 K, $u(x)$ = 0.0001, and the expanded uncertainties for densities $U(\rho)$ and excess molar volumes $U(V^E)$ are 3·10^{-5} g·cm^{-3} and 0.003 cm^3·mol^{-1}, respectively (level of confidence = 0.95).

where η_0 (mPa·s), B (K), and T_0 (K) are empirical constants.[28,30] The best fitted parameters have been listed in Table 6.

From Table 5, the viscosity values fall in the range from (6.824 to 78.29) mPa·s. The viscosity of each IL decreases sharply when the temperature increase from (293.15 to 343.15) K. It suggests that the increase of temperature could significantly reduce the ILs' internal resistance to flow. And the internal resistance is mainly derived from the cation−anion interaction of ILs, including hydrogen bonds and electrostatic and van der Waals' forces.[31,32] At the same temperature, the viscosities of ILs decrease in the following order: [Bmim]Cl/$AlCl_3$ (x = 0.5455) > [Bmim]Cl/$AlCl_3$ (x = 0.5833) > [Bmim]Cl/$AlCl_3$ (x = 0.6154) > [Bmim]Cl/$AlCl_3$ (x = 0.6429) > [Bmim]Cl/$AlCl_3$ (x = 0.6667), and [H_1mim]Cl/$AlCl_3$ (x = 0.6429) > [H_1mim]Cl/$AlCl_3$ (x = 0.6667), showing that an increased molar concentration of $[Al_2Cl_7]^-$ reduces the viscosity. As shown in Figure 3 and Table 4, the cation−anion interaction energy and hydrogen bond length of ion pairs follow the order: [Bmim][Al_2Cl_7] < [Bmim][$AlCl_4$], and [H_1mim][Al_2Cl_7] < [H_1mim][$AlCl_4$]. For example, the interaction energy of [Bmim][Al_2Cl_7] and [Bmim][$AlCl_4$] is 270.61 KJ·mol^{-1} and 290.98 KJ·mol^{-1}, respectively. The distances of hydrogen bonds, C2−H···Cl (2.588 Å) and C7−H···Cl (2.697 Å) in [Bmim][$AlCl_4$] are shorter than the corresponding bonds in [Bmim][Al_2Cl_7], which implies that there exists stronger hydrogen bonding in [Bmim][$AlCl_4$].[33,34] Based on above results, it is proper to state that the internal resistance of ILs becomes weaker as the concentration of $[Al_2Cl_7]^-$ increases.

The viscosities of chloroaluminate ILs are also greatly affected by the structure of cation. It can be observed from the experimental data that the viscosity of [H_1mim]Cl/$AlCl_3$ is much higher than that of [Bmim]Cl/$AlCl_3$ at the same temperature and apparent mole fraction of $AlCl_3$. As presented in Figure 3 and Table 4, the interaction energy between ion pairs increases in the order, [Bmim][$AlCl_4$] < [H_1mim][$AlCl_4$], and [Bmim][Al_2Cl_7] < [H_1mim][Al_2Cl_7]. Moreover, the distances of hydrogen bonds, C2−H···Cl and N1−H···Cl in $[H_1mim]^+$-based ion pairs are shorter compared with those in $[Bmim]^+$-based ones when the anions are the same. It shows that $[H_1mim]^+$-based ILs have stronger interaction energy and hydrogen bonding, leading to the higher viscosity of [H_1mim]Cl/$AlCl_3$.

3.3. Electrical Conductivity. Table 7 lists the electrical conductivities, κ, of Lewis acidic [Bmim]Cl/$AlCl_3$ and [H_1mim]Cl/$AlCl_3$ ILs recorded from (298.15 to 343.15) K. The temperature dependency of electrical conductivity is shown in Figure 5. The experimental data have been fitted by the VFT equation:[28,35]

$$\kappa = \kappa_0 \exp(-B/(T - T_0)) \quad (5)$$

where κ_0 (S·cm^{-1}), B (K), and T_0 (K) are adjustable parameters. The values of best fitted parameters are presented in Table 8.

Ionic conductivity is a key factor to the application of ILs in electrochemistry. The chloroaluminate ILs used in this study have higher electrical conductivities (>15 mS·cm^{-1} at 338.15 K) than many traditional ILs.[28,35] As the temperature rises, the electrical conductivities of [Bmim]Cl/$AlCl_3$ and [H_1mim]Cl/$AlCl_3$ increase rapidly. It implies that the charge transfer between ions is prone to conduct once the attractive interaction in ILs becomes weaker with increasing temperature.

Shown in Table 7 and Figure 5, the electrical conductivities of [H_1mim]Cl/$AlCl_3$ are lower than those of [Bmim]Cl/$AlCl_3$ when these ILs contain the same apparent mole fraction of $AlCl_3$ at each studied temperature. As revealed in Sections 3.1 and 3.2, stronger cation−anion interaction and hydrogen

dx.doi.org/10.1021/je3004904 | J. Chem. Eng. Data 2013, 58, 32−42

Table 12. Experimental Viscosity η (mPa·s), and Viscosity Deviation, $\Delta\eta$ (mPa·s), for the Binary Mixture of [Bmim][Al_2Cl_7] (1) + [Bmim][$AlCl_4$] (2)[a]

	T/K					
x_1	293.15	303.15	313.15	323.15	333.15	343.15
			η/mPa·s			
0.0000	41.63	28.33	20.76	16.06	12.95	10.78
0.1001	38.28	26.36	19.48	15.16	12.28	10.26
0.1998	34.99	24.32	18.08	14.13	11.47	9.626
0.3003	32.26	22.62	16.92	13.29	10.83	9.087
0.4002	30.34	21.36	16.01	12.60	10.28	8.633
0.5009	28.34	20.20	15.28	12.09	9.902	8.341
0.6001	26.89	19.33	14.59	11.55	9.492	8.011
0.7000	25.31	18.29	13.96	11.12	9.149	7.729
0.8005	24.35	17.68	13.53	10.78	8.881	7.499
0.8996	23.44	17.10	13.12	10.48	8.629	7.209
1.0000	22.54	16.73	12.87	10.17	8.231	6.824
			$\Delta\eta$/mPa·s			
0.1001	−1.44	−0.81	−0.49	−0.31	−0.20	−0.12
0.1998	−2.83	−1.69	−1.10	−0.75	−0.54	−0.36
0.3003	−3.64	−2.23	−1.47	−1.00	−0.70	−0.51
0.4002	−3.65	−2.33	−1.59	−1.10	−0.78	−0.56
0.5009	−3.73	−2.32	−1.53	−1.02	−0.68	−0.46
0.6001	−3.28	−2.04	−1.44	−0.98	−0.63	−0.40
0.7000	−2.96	−1.92	−1.28	−0.82	−0.50	−0.28
0.8005	−2.00	−1.36	−0.91	−0.57	−0.29	−0.11
0.8996	−1.02	−0.79	−0.54	−0.28	−0.08	−0.01

[a]The composition x_1 is the mole fraction of [Bmim][Al_2Cl_7] in the binary mixture. Standard uncertainties u are $u(T)$ = 0.01 K, $u(x)$ = 0.0001, and the relative expanded uncertainties for the viscosities $U_r(\eta)$ and viscosity deviations $U_r(\Delta\eta)$ are 0.005 and 0.02, respectively (level of confidence = 0.95).

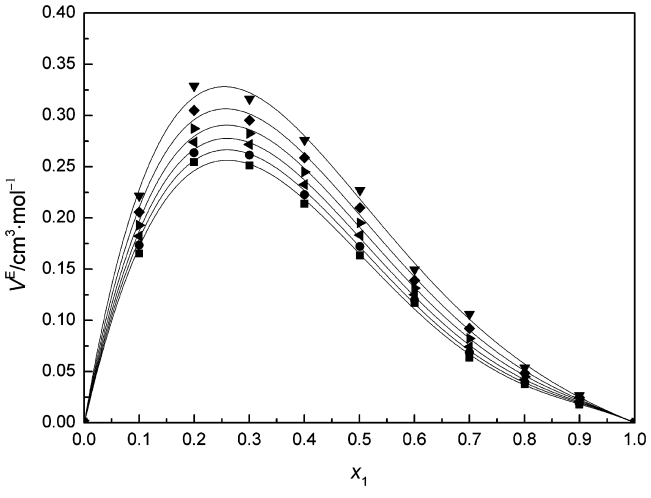

Figure 7. Excess molar volume V^E vs mole fraction x_1 of [Bmim][Al_2Cl_7] for [Bmim][Al_2Cl_7] (1) + [Bmim][$AlCl_4$] (2): ■, 293.15 K; ●, 303.15 K; ◀, 313.15 K; ▶, 323.15 K; ◆, 333.15 K; ▼, 343.15 K. The solid curves are calculated with the Redlich−Kister equation, and the symbols represent experimental values.

bonding exist between [Hmim]$^+$-based ion pairs. Hence, it can be explained that relatively strong interaction force in [H_1mim]Cl/$AlCl_3$ weakens the movement of ions, resulting in the lower ionic conductivity.

For the ILs with different molar compositions, the electrical conductivities follow the order: [Bmim]Cl/$AlCl_3$ (x = 0.5455) > [Bmim]Cl/$AlCl_3$ (x = 0.5833) > [Bmim]Cl/$AlCl_3$ (x = 0.6154) > [Bmim]Cl/$AlCl_3$ (x = 0.6429) > [Bmim]Cl/$AlCl_3$ (x = 0.6667). Different from viscosity, the ionic conductivity of [Bmim]Cl/$AlCl_3$ increases with increasing molar concentration of $[AlCl_4]^-$ anions. Although [Bmim][$AlCl_4$] has stronger cation−anion interaction and hydrogen bonding than [Bmim][Al_2Cl_7], $[AlCl_4]^-$ has a smaller volume and higher geometric symmetry than $[Al_2Cl_7]^-$. In consideration of these facts, it can be inferred that the structural features make $[AlCl_4]^-$ more conductive in [Bmim]Cl/$AlCl_3$ at the same conditions. Therefore, this is probably a main reason why the electrical conductivity of [Bmim]Cl/$AlCl_3$ decreases as the apparent mole fraction of $AlCl_3$ increases.

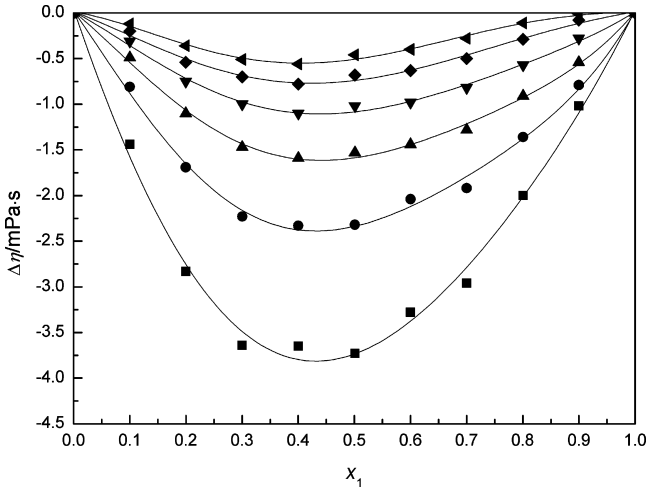

Figure 8. Viscosity deviation $\Delta\eta$ vs mole fraction x_1 of [Bmim][Al_2Cl_7] for [Bmim][Al_2Cl_7] (1) + [Bmim][$AlCl_4$] (2): ■, 293.15 K; ●, 303.15 K; ▲, 313.15 K; ▼, 323.15 K; ◆, 333.15 K; ◀, 343.15 K. The solid curves are calculated with the Redlich−Kister equation, and the symbols represent experimental values.

Compared with [Bmim]Cl/$AlCl_3$, the electrical conductivities of [H_1mim]Cl/$AlCl_3$ with different molar compositions appear to be in an opposite trend, [H_1mim]Cl/$AlCl_3$ (x = 0.6429) < [H_1mim]Cl/$AlCl_3$ (x = 0.6667). As analyzed above, an increase in the molar concentration of $[AlCl_4]^-$ has the potential to enhance the ionic conductivity of [H_1mim]Cl/$AlCl_3$. However, it should be noted that a larger viscosity difference exists in the studied [H_1mim]Cl/$AlCl_3$ ILs. For example, the viscosity difference between [H_1mim]Cl/$AlCl_3$ (x = 0.6429) and [H_1mim]Cl/$AlCl_3$ (x = 0.6667) is 27.49 mPa·s at 293.15 K, compared to 1.84 mPa·s between the viscosity of [Bmim]Cl/$AlCl_3$ (x = 0.6429) and [Bmim]Cl/$AlCl_3$ (x = 0.6667) at 293.15 K. It suggests that the internal resistance and cation−anion interaction of [H_1mim]Cl/$AlCl_3$ decreases at a faster rate with increasing molar concentration of $[Al_2Cl_7]^-$. Accordingly, it can be concluded that the enhanced movement of ions becomes a dominant factor for the increasing conductivity in [H_1mim]Cl/$AlCl_3$.

The electrical conductivity discussed above reflects the sum of effective ions for charge transfer in ILs, while each IL has a different ion concentration. Therefore, the molar conductivity, Λ, is indispensable in the study of ion mobility for ionic conductivity. On the basis of electrical conductivity and density values, the molar conductivities of Lewis acidic [Bmim]Cl/$AlCl_3$ and [H_1mim]Cl/$AlCl_3$ have been calculated by

$$\Lambda = \kappa \cdot M \cdot \rho^{-1} \quad (6)$$

dx.doi.org/10.1021/je3004904 | J. Chem. Eng. Data 2013, 58, 32−42

Table 13. Coefficients of the Redlich−Kister Equation for V^E and $\Delta\eta$ of the [Bmim][Al_2Cl_7] (1) + [Bmim][$AlCl_4$] (2) System

property	T/K	A_0	A_1	A_2	A_3	σ
V^E/cm^3·mol^{-1}	293.15	0.6688	−1.1572	0.5743	0.1895	0.0047
	303.15	0.6963	−1.1872	0.6065	0.1630	0.0040
	313.15	0.7300	−1.2148	0.6401	0.1267	0.0036
	323.15	0.7687	−1.2449	0.6840	0.0803	0.0038
	333.15	0.8159	−1.2812	0.7370	0.0150	0.0050
	343.15	0.8809	−1.3349	0.7984	−0.0557	0.0064
$\Delta\eta$/mPa·s	293.15	−15.22	4.84	1.77	−2.78	0.1199
	303.15	−9.51	2.98	0.62	−4.32	0.0693
	313.15	−6.45	1.97	0.92	−3.50	0.0422
	323.15	−4.44	1.51	1.55	−1.97	0.0378
	333.15	−3.07	1.55	2.08	−1.08	0.0379
	343.15	−2.09	1.73	2.00	−1.48	0.0245

where M represents the molar mass of chloroaluminate IL. The data of molar conductivity obtained at the temperature of (298.15 to 343.15) K are given in Table 9. For illustration, Figure 6 shows the temperature dependency of molar conductivity of [Bmim]Cl/$AlCl_3$ (x = 0.6667) and [H_1mim]Cl/$AlCl_3$ (x = 0.6667) according to the VFT equation:[28,30]

$$\Lambda = \Lambda_0 \exp(-B/(T - T_0)) \tag{7}$$

where Λ_0 (S·cm^2·mol^{-1}), T (K), and T_0 (K) are adjustable parameters. The values of best fitted parameters have been listed in Table 10.

As Table 9 shows, the molar conductivities of the studied ILs increase when temperature rises, indicating that the ion mobility is highly depended on the temperature. Meanwhile, it is apparent that the increased apparent mole fraction of $AlCl_3$ promotes the ILs' molar conductivity at the same conditions. Mainly due to the rapid increase in electrical conductivity, the ion mobility of [H_1mim]Cl/$AlCl_3$ changes more than that of [Bmim]Cl/$AlCl_3$ as a function of molar composition.

At the same temperatures, the molar conductivities of ILs follow the order: [Bmim]Cl/$AlCl_3$ (x = 0.6429) > [H_1mim]Cl/$AlCl_3$ (x = 0.6429), and [Bmim]Cl/$AlCl_3$ (x = 0.6667) > [H_1mim]Cl/$AlCl_3$ (x = 0.6667). From above discussion, it can be concluded that the relatively weak cation−anion interaction and structural features of [Bmim]Cl/$AlCl_3$ result in not only low packing density of ions, but also higher ionic charge transfer. This may explain the fact that [Bmim]Cl/$AlCl_3$ has a higher ion mobility than [H_1mim]Cl/$AlCl_3$ when they contain the same apparent mole fraction of $AlCl_3$.

3.4. Excess Molar Volume and Viscosity Deviation. Considering that Lewis acidic chloroaluminate ILs can be seen as the binary mixtures of [Rmim][Al_2Cl_7] and [Rmim][$AlCl_4$], it is necessary to evaluate how ideal these ILs are by calculating excess volume and viscosity deviation. Pure [Rmim][Al_2Cl_7] and [Rmim][$AlCl_4$] can be obtained when the apparent mole fraction of $AlCl_3$ is 0.6667 and 0.5000, respectively. In this section, the densities and viscosities for the binary system of [Bmim]Cl/$AlCl_3$ (x = 0.6667) and [Bmim]Cl/$AlCl_3$ (x = 0.5000) were measured from (293.15 to 343.15) K. The values of these properties are presented in Tables 11 and 12. Compared to the experimental data shown in Sections 3.1 and 3.2, the densities and viscosities of these mixtures change in the same way as a function of temperature and molar composition. To facilitate the discussion, [Bmim]Cl/$AlCl_3$ (x = 0.6667) and [Bmim]Cl/$AlCl_3$ (x = 0.5000) are expressed by [Bmim][Al_2Cl_7] and [Bmim][$AlCl_4$] in the following content, respectively.

The excess molar volumes V^E and viscosity deviations $\Delta\eta$ have been calculated by the following equations:[36,37]

$$V^E = \frac{x_1M_1 + x_2M_2}{\rho} - \left(\frac{x_1M_1}{\rho_1} + \frac{x_2M_2}{\rho_2}\right) \tag{8}$$

$$\Delta\eta = \eta - (x_1\eta_1 + x_2\eta_2) \tag{9}$$

where ρ and η are the density and viscosity of mixtures; x_1 and x_2 are mole fractions; M_1 and M_2 are molar masses; ρ_1 and ρ_2 are densities; and η_1 and η_2 are the viscosities of [Bmim][Al_2Cl_7] (1) and [Bmim][$AlCl_4$] (2), respectively.

All of the experimental values of V^E and $\Delta\eta$ were fitted according to the Redlich−Kister polynomial equation:

$$Y = x_1(1 - x_1)\sum_{i=0}^{k} A_i(2x_1 - 1)^i \tag{10}$$

in which Y is V^E or $\Delta\eta$, A_i are adjustable parameters, and x_1 is the mole fraction of [Bmim][Al_2Cl_7]. The standard deviation σ was determined by the following equation:[38,39]

$$\sigma(Y) = \left[\frac{\sum (Y_{cal} - Y_{exp})^2}{n - p}\right]^{1/2} \tag{11}$$

where n is the number of experimental data, and p is the number of coefficients of eq 10.

Tables 11 and 12 also list the data of excess molar volume and viscosity deviation. The excess molar volume and viscosity deviation versus mole fraction of [Bmim][Al_2Cl_7] are plotted in Figures 7 and 8, respectively. The values of parameters A_i and standard deviations σ are shown in Table 13.

From Figure 7, the excess molar volumes for the mixtures of [Bmim][Al_2Cl_7] and [Bmim][$AlCl_4$] are positive at all of the studied temperatures and mole fractions. The excess molar volume increases when temperature increases from (293.15 to 343.15) K. The maximum value is found at x_1 = 0.2. It indicates that a less efficient packing and/or weaker attractive interaction occurs among ions after [Bmim][Al_2Cl_7] and [Bmim][$AlCl_4$] are mixed. Meanwhile, it can be seen from Figure 8 that the values of viscosity deviation are negative, and the minimum is at x_1 = 0.4 or 0.5 over the whole range of experimental conditions. The viscosity deviations also increase as temperature rises.

4. CONCLUSIONS

In this work, the densities, viscosities, and electrical conductivities of Lewis acidic chloroaluminate ILs, [Bmim]-

dx.doi.org/10.1021/je3004904 | J. Chem. Eng. Data 2013, 58, 32−42

$Cl/AlCl_3$ and $[H_1mim]Cl/AlCl_3$ with different apparent mole fractions of $AlCl_3$ have been investigated from (293.15 to 343.15) K. The excess molar volumes and viscosity deviations for the binary mixtures of $[Bmim][Al_2Cl_7]$ and $[Bmim][AlCl_4]$ were also determined. All of the experimental values were fitted according to the empirical equations. It showed that $[H_1mim]$-$Cl/AlCl_3$ was denser, more viscous, and less conductive than $[Bmim]Cl/AlCl_3$ at the same conditions. Moreover, the properties of ILs have been investigated with the variation of molar compositions. According to the optimized geometries and structural parameters of ion pairs obtained by the DFT method, it can be inferred that the structural symmetry, cation−anion interaction, and hydrogen bonds of chloroaluminate ILs have significant effects on the studied physicochemical properties. For $[Bmim]Cl/AlCl_3$ and $[H_1mim]Cl/AlCl_3$, the difference in the values of density, viscosity, and conductivity were analyzed from above simulation results. It is expected that the present research may find important application in the development of these ILs as electrolytes and catalysts.

AUTHOR INFORMATION

Corresponding Author

*E-mail: xmlu@home.ipe.ac.cn. Tel.: +86 10 82544800. Fax: +86 10 62558174.

Funding

This work was supported financially by the National Basic Research Program of China (2009CB219901), National Key Technology Research and Development Program of the Ministry of Science and Technology of China (2012BAF03B01), and National Natural Science Foundation of China (21036007, 51274181).

Notes

The authors declare no competing financial interest.

ACKNOWLEDGMENTS

The authors gratefully acknowledge Prof. Suojiang Zhang, Dr. Muhammad Yaseen, and Dr. Qing Zhou for their guidance and meaningful discussion in this work.

REFERENCES

(1) Welton, T. Room-temperature ionic liquids. Solvents for synthesis and catalysis. *Chem. Rev.* **1999**, *99*, 2071−2083.

(2) Binnemans, K. Ionic liquid crystals. *Chem. Rev.* **2005**, *105*, 4148−4204.

(3) Marciniak, A.; Karczemna, E. Influence of cation structure on binary liquid-liquid equilibria for systems containing ionic liquids based on trifluoromethanesulfonate anion with hydrocarbons. *J. Phys. Chem. B* **2010**, *114*, 5470−5474.

(4) Wang, C.; Luo, H.; Li, H.; Dai, S. Direct UV-spectroscopic measurement of selected ionic-liquid vapors. *Phys. Chem. Chem. Phys.* **2010**, *12*, 7246−7250.

(5) Greaves, T. L.; Drummond, C. J. Protic ionic liquids: properties and applications. *Chem. Rev.* **2008**, *108*, 206−237.

(6) Galiński, M.; Lewandowski, A.; Stępniak, I. Ionic liquids as electrolytes. *Electrochim. Acta* **2006**, *51*, 5567−5580.

(7) Dupont, J.; de Souza, R. F.; Suarez, P. A. Z. Ionic liquid (molten salt) phase organometallic catalysis. *Chem. Rev.* **2002**, *102*, 3667−3692.

(8) Han, X.; Armstrong, D. W. Ionic liquids in separations. *Acc. Chem. Res.* **2007**, *40*, 1079−1086.

(9) Miao, W.; Chan, T. H. Exploration of ionic liquids as soluble supports for organic synthesis. Demonstration with a Suzuki coupling reaction. *Org. Lett.* **2003**, *5*, 5003−5005.

(10) Hurley, F. H.; Wier, T. P. The electrodeposition of aluminum from nonaqueous solutions at room temperature. *J. Electrochem. Soc.* **1951**, *98*, 207−212.

(11) Trulove, P. C.; Osteryoung, R. A. Proton speciation in ambient-temperature chloroaluminate ionic liquids. *Inorg. Chem.* **1992**, *31*, 3980−3985.

(12) Yadav, J. S.; Reddy, B. V. S.; Reddy, M. S.; Niranjan, N.; Prasad, A. R. Lewis acidic chloroaluminate ionic liquids: novel reaction media for the synthesis of 4-chloropyrans. *Eur. J. Org. Chem.* **2003**, 1779−1783.

(13) Kemperman, G. J.; Roeters, T. A.; Hilberink, P. W. Cleavage of aromatic methyl ethers by chloroaluminate ionic liquid reagents. *Eur. J. Org. Chem.* **2003**, 1681−1686.

(14) Lang, C. M.; Kim, K.; Guerra, L.; Kohl, P. A. Cation electrochemical stability in chloroaluminate ionic liquids. *J. Phys. Chem. B* **2005**, *109*, 19454−19462.

(15) Salanne, M.; Siqueira, L. J. A.; Seitsonen, A. P.; Madden, P. A.; Kirchner, B. From molten salts to room temperature ionic liquids: simulation studies on chloroaluminate systems. *Faraday Discuss.* **2012**, *154*, 171−188.

(16) Abbott, A. P.; Qiu, F.; Abood, H. M. A.; Rostom Ali, M.; Ryder, K. S. Double layer, diluent and anode effects upon the electrodeposition of aluminium from chloroaluminate based ionic liquids. *Phys. Chem. Chem. Phys.* **2010**, *12*, 1862−1872.

(17) Jiang, T.; Chollier Brym, M. J.; Dubé, G.; Lasia, A.; Brisard, G. M. Electrodeposition of aluminium from ionic liquids: Part II−studies on the electrodeposition of aluminum from aluminum chloride ($AlCl_3$)−trimethylphenylammonium chloride (TMPAC) ionic liquids. *Surf. Coat. Technol.* **2006**, *201*, 10−18.

(18) Jiang, T.; Chollier Brym, M. J.; Dubé, G.; Lasia, A.; Brisard, G. M. Electrodeposition of aluminium from ionic liquids: Part I−electrodeposition and surface morphology of aluminium from aluminium chloride ($AlCl_3$)−1-ethyl-3-methylimidazolium chloride ([EMIm]Cl) ionic liquids. *Surf. Coat. Technol.* **2006**, *201*, 1−9.

(19) Abbott, A. P.; Eardley, C. A.; Farley, N. R. S.; Griffith, G. A.; Pratt, A. Eletrodeposition of aluminium and aluminium/platinum alloys from $AlCl_3$/benzyltrimethylammonium chloride room temperature ionic liquids. *J. Appl. Electrochem.* **2001**, *31*, 1345−1350.

(20) Zein El Abedin, S.; Giridhar, P.; Schwab, P.; Endres, F. Electrodeposition of nanocrystalline aluminium from a chloroaluminate ionic liquid. *Electrochem. Commun.* **2010**, *12*, 1084−1086.

(21) Snelders, D. J. M.; Dyson, P. J. Efficient synthesis of β-chlorovinylketones from acetylene in chloroaluminate ionic liquids. *Org. Lett.* **2011**, *13*, 4048−4051.

(22) Yue, G.; Zhang, S.; Zhu, Y.; Lu, X.; Li, S.; Li, Z. A promising method for electrodeposition of aluminium on stainless steel in ionic liquid. *AIChE J.* **2009**, *55*, 783−796.

(23) Yue, G.; Lu, X.; Zhu, Y.; Zhang, X.; Zhang, S. Surface morphology, crystal structure and orientation of aluminium coatings electrodeposited on mild steel in ionic liquid. *Chem. Eng. J.* **2009**, *147*, 79−86.

(24) Fannin, A. A.; Floreani, D. A.; King, L. A.; Landers, J. S.; Piersma, B. J.; Stech, D. J.; Vaughn, R. L.; Wilkes, J. S.; Williams, J. L. Properties of 1,3-dialkylimidazolium chloride-aluminium chloride ionic liquids. 2. Phrase transitions, density, electrical conductivities, and viscosities. *J. Phys. Chem.* **1984**, *88*, 2614−2621.

(25) Wilkes, J. S.; Levisky, J. A.; Wilson, R. A.; Hussey, C. L. Dialkylimidazolium chloroaluminate melts: a new class of room-temperature ionic liquids for electrochemistry, spectroscopy, and synthesis. *Inorg. Chem.* **1982**, *21*, 1263−1264.

(26) Huddleston, J. G.; Visser, A. E.; Reichert, W. M.; Willauer, H. D.; Broker, G. A.; Rogers, R. D. Characterization and comparison of hydrophilic and hydrophobic room temperature ionic liquids incorporating the imidazolium cation. *Green Chem.* **2001**, *3*, 156−164.

(27) Ohno, H.; Yoshizawa, M. Ion conductive characteristics of ionic liquids prepared by neutralization of alkylimidazoles. *Solid State Ionics* **2002**, *154/155*, 303−309.

(28) Liu, Q. S.; Yang, M.; Li, P. P.; Sun, S. S.; Welz-Biermann, U.; Tan, Z. C.; Zhang, Q. G. Physicochemical properties of ionic liquids $[C_3py][NTf_2]$ and $[C_6py][NTf_2]$. *J. Chem. Eng. Data* **2011**, *56*, 4094−4101.

(29) Ghatee, M. H.; Zare, M.; Moosavi, F.; Zolghadr, A. R. Temperature-dependent density and viscosity of the ionic liquids 1-alkyl-3-methylimidazolium iodides: experiment and molecular dynamics simulation. *J. Chem. Eng. Data* **2010**, *55*, 3084−3088.
(30) Tokuda, H.; Hayamizu, K.; Ishii, K.; Abu Bin Hasan Susan, M.; Watanabe, M. Physicochemical properties and structures of room temperature ionic liquids. 2. Variation of alkyl chain length in imidazolium cation. *J. Phys. Chem. B* **2005**, *109*, 6103−6110.
(31) Yu, G.; Zhang, S. Insight into the cation-anion interaction in 1,1,3,3-tetramethylguanidinium lactate ionic liquid. *Fluid Phase Equilib.* **2007**, *255*, 86−92.
(32) Xuan, X.; Guo, M.; Pei, Y.; Zheng, Y. Theoretical study on cation-anion interaction and vibration spectra of 1-allyl-3-methylimidazolium-based ionic liquids. *Spectrochim. Acta, Part A* **2011**, *78*, 1492−1499.
(33) Dong, K.; Zhang, S.; Wang, D.; Yao, X. Hydrogen bonds in imidazolium ionic liquids. *J. Phys. Chem. A* **2006**, *110*, 9775−9782.
(34) Acevedo, O. Determination of local effects for chloroaluminate ionic liquids on Diels-Alder reactions. *J. Mol. Graph. Model.* **2009**, *28*, 95−101.
(35) Wu, T. Y.; Su, S. G.; Gung, S. T.; Lin, M. W.; Lin, Y. C.; Lai, C. A.; Sun, I. W. Ionic liquids containing an alkyl sulfate group as potential electrolytes. *Electrochim. Acta* **2010**, *55*, 4475−4482.
(36) Pal, A.; Dass, G. Excess molar volumes and viscosities for binary liquid mixtures of 2-propoxyethanol and of 2-isopropoxyethanol with methanol, 1-propanol, 2-propanol, and 1-pentanol at 298.15 K. *J. Chem. Eng. Data* **2000**, *45*, 693−698.
(37) Weng, W. L. Densities and viscosities for binary mixtures of butylamine with aliphatic alcohols. *J. Chem. Eng. Data* **2000**, *45*, 606−609.
(38) Serrano, L.; Silva, J. A.; Farelo, F. Densities and viscosities of binary and ternary liquid systems containing xylenes. *J. Chem. Eng. Data* **1990**, *35*, 288−291.
(39) Nath, J.; Pandey, J. G. Excess molar volumes of heptan-1-ol + pentane, + hexane, + heptane, + octane, and + 2,2,4-trimethylpentane at T = 293.15 K. *J. Chem. Eng. Data* **1997**, *42*, 1137−1139.